CO Adsorption Isotherms on Ice by Fourier Transform Infrared Spectroscopy and New Insights of the Ice Surface from Quantum ab Initio Investigations

A. Allouche,*,[1] P. Verlaque, and J. Pourcin

Physique des Interactions Ioniques et Moléculaires, Université de Provence−CNRS (UMR 6633), Campus Universitaire de Saint Jérôme, Service 541, 13397 Marseille Cedex 20, France

Received: March 10, 1997; In Final Form: October 13, 1997[⊗]

Various ice samples are prepared from highly concentrated H_2O/Ar matrixes submitted to various annealing treatments. Each of these samples corresponds to a different stage in the solid organization from amorphous to nanocrystalline clusters. The type II isotherms are drawn from a 0.1 to a few monolayers surface coverage in the 43−48 K temperature range as a function of the integrated absorbance of the carbon monoxide (CO) vibrational mode, measured by FTIR spectroscopy, vs the CO equilibrium pressure. In the frame of the Brunauer, Emmett, and Teller (BET) model the mean enthalpy of adsorption of the first CO monolayer is evaluated to be about 10 kJ mol^{-1} and is independent of the history of the ice surfaces. The quantum modeling on a perfect ice surface leads to adsorption energies in good agreement with experimental results for an isolated admolecule as well as for the monolayer. The CO adsorbs perpendicularly to the surface plane, and the two orientations of CO or OC are energetically equivalent. Adsorption on a surface defect modeled as a hole indicates hydrogen bonding between the admolecule and the substrate. Comparing experimental and quantum results, we may conclude that the CO molecule sees the ice surface as covered by protons that make the adsorption dynamic process insensitive to the presence of surface defects.

1. Introduction

The study of chemical processes on the surface of ice has been the focus of attention over the past few years primarily because of a lack of suitable information on the mechanism and rate of heterogeneous reactions of interest in the stratosphere and the troposphere.[2] The main difficulty of these kinds of studies lies in the poor knowledge of the structure of the substrate's surface. Nevertheless, from a theoretical point of view, some progress has been achieved recently, in particular by van Hove's[3] and Pisani's[4] groups.

Delvin's group has proposed the most extensive and important contribution based on a combination of ice growth experimental protocols and surface structure characterization by infrared spectroscopy.[5] Some hypotheses on ice surface structure were proposed using CF_4 as a probe molecule and Monte Carlo simulation.[5f] They have established that the equilibrium state of ice obtained by deposition on a cold substrate or condensation on the windows of a cooled cell appears as microporous amorphous solids or monocrystalline clusters of randomly distributed free surfaces. By adequately selecting the adsorbed molecule, Devlin and co-workers were able to investigate the ice surface structure and obtain information on its short- and long-range order.

More recently, Roberts and co-workers[6] conducted a study on a rather large panel of molecules adsorbed on a thin film of ice. From the variety of the chemical properties of these molecules they were able to derive information relevant to the ice surface.

It has been demonstrated that the vibrational spectra of carbon monoxide (CO) measured by infrared spectroscopy provide a good probe of a great number of solid surfaces such as surfaces of metals and metal oxides,[7] ionic solids,[8] and zeolites.[9] Because of its small dipole moment and its poor affinity for water, CO does not significantly perturb the ice surface. Also, its very good spectral response in infrared spectroscopy makes it highly sensitive to a surface field perturbation, thus providing useful information on the admolecule−substrate interaction. To probe the ice surface by a nondestructive method, we propose evaluating the physisorption binding energy of CO on various ice surfaces monitored by FTIR spectroscopy.

The present paper is organized as follows. In the Experimental Section we shall describe the method used to generate ice samples of different degrees of organization and, for each of them, the application of infrared spectra to the calculation of the mean enthalpy of adsorption of the first CO monolayer.

Quantum calculations are then performed to estimate the adsorption energy on a perfect surface. Two different ab initio methods are applied respectively to an isolated molecule on the surface and to the monolayer. Then a model defect on the surface is used to analyze the defect-induced perturbation on the ice−molecule interaction. In conclusion, we propose a tentative new insight on the ice surface structure.

2. Experimental Section

2.1. Ice Sample Preparation and CO Adsorption. Our aim being to study the thermodynamic of CO adsorption on ice, we opted for an experimental technique in which we tried to satisfy two drastic requirements: (i) use of icy samples at low temperature, presenting large surface areas to achieve spectra with the best possible signal-to-noise ratio and (ii) use of a cryostat containing a pressure gauge to allow measurements in the 10^{-4}−1 Pa limited pressure range in order to avoid damage by accidental cooling of the KBr windows.

The CO physical properties are reported in Table 1, and its

[⊗] Abstract published in *Advance ACS Abstracts,* November 15, 1997.

S1089-5647(97)00877-8 CCC: $15.00
Published on Web 01/01/1998

TABLE 1: CO Physical Properties

triple point [43] K, kPa	critical *T* K	critical *P* kPa	saturation pressure of α-CO[a,44] A	B
68.1, 15.4	132.9	3498.7	433.71	10.62

[a] In the 55−60 K range.

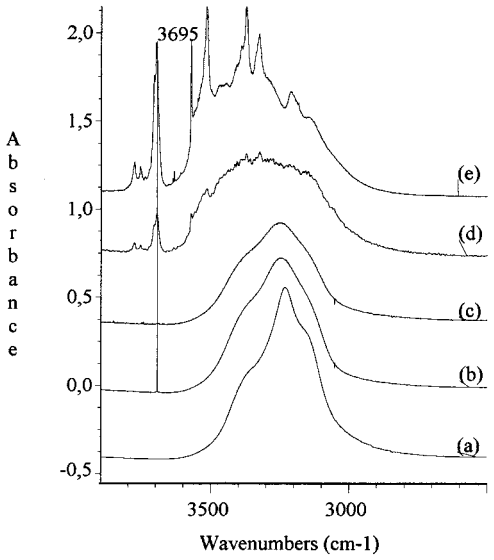

Figure 1. Infrared spectra for (e) H_2O in a $^1/_{50}$ concentrated argon matrix deposited and recorded at 10 K; (d and c) the same sample recorded at 30 and 85 K; (b) sample at 43 K after annealing at 85 K; (a) crystalline ice absorption band after annealing at 160 K for comparison. The dangling mode is reported at 3695 cm^{-1}. Spectra are offset on the vertical axis.

saturation pressure has been calculated in the 37−48 K range from an extrapolation of Clapeyron's law coefficients measured in the 55−60 K range (Table 1).

We chose to prepare the substrate at a rate of 2−2.5 mmol h^{-1} by continuous vacuum deposition of an H_2O/Ar gaseous mixture on a CsBr vertical substrate cooled to 10 K by a CTI Model 21 closed-cycle helium refrigerator. The coldfinger was surrounded by a radiation shield maintained at 77 K. Temperature measurements, stabilization, and control were achieved by a D.R.C. 84C, Lake Shore Cryotonic Inc. controller. Argon material was chosen to follow the ice production from the well-known concentrated H_2O in Ar matrix spectra.[10] The concentration of the gas mixture was established using a standard manometric procedure in a separate vessel and was introduced into the cryostat through a stainless steel tube. In Figure 1a, the unannealed sample infrared spectrum, after deposition, is similar to the spectrum of water in matrix isolation.[10] Two peaks around 3756 and 3638 cm^{-1} were assigned to the ν_3 (B_1) and ν_1 (A_1) vibrational stretching modes of isolated H_2O, and that at 3695 cm^{-1} was assigned to the vibrational frequency of the free OH stretch (Devlin's dangling mode) in interaction with the surrounding Ar atoms. The multimers appeared as broad and overlapped peaks between 3550 and 2800 cm^{-1}. When the sample was annealed at 43 K from the deposition temperature, the light became more and more scattered and we observed a strong reduction of the sample transparency. With the temperature maintained at 45 K for 1 h, the solid again became transparent while the spectral feature exhibited dramatic changes. The single-donor and double-donor OH stretching modes (the bulk modes of ice) appeared as a broad overlapped band around 3200 cm^{-1}, 500 cm^{-1} downshifted from the stretching modes of the free water molecule. The O−H

TABLE 2: Summary of Measured Adsorption Energies for Thin Films of Ice in Different Solid Organizations at 43 and 48 K

surfaces	*T* (K)	*d* (μm)	A_0 (cm^{-1})	*c*	$-(\epsilon' - \epsilon)$ (kJ mol^{-1})	adsorption energies $-\epsilon$ (kJ mol^{-1})
S1	43	0.43	0.45	579	2.26	9.75
S2	43	0.37	0.40	374	2.12	9.69
S3	43	0.35	0.79	397	2.14	9.72
S5	45	0.65	0.08	585	2.42	10.03
S3	48	0.35	0.16	858	2.69	10.31

dangling mode remains as a small single peak at 3694 cm^{-1}. At 45 K, the Ar saturation pressure lies around 1.3 Pa and most of the rare gas is outgassing from the sample under the base pressure of the cryostat (10^{-5} Pa). Annealing to 85 K simply produced a large decrease of the dangling mode intensity, without measurable frequency shift, and a strong narrowing of its band shape. It appeared as a very weak single peak centered at 3694 cm^{-1} with a full width at half-maximum of about 15 cm^{-1}. This result must be compared with that previously published by Devlin et al.[11] showing that the O−H dangling band for three-coordinate surface water molecules for crystalline ice clusters is found to appear as a narrow peak at 3692 cm^{-1}. This let us assume a crystalline structure for our sample. At 85 K, we also observed (Figure 1c) a narrowing of the spectral feature corresponding to the O−H bulk modes with a strong central peak centered at 3251 cm^{-1} surrounded by two shoulders of lower intensities and a dramatic decrease of the H−O−H bend at 1660 cm^{-1}. Parts b and a of Figure 1 give the spectra of the 85 K annealed sample held at 43 K in comparison with that of the same 160 K annealed sample. Perhaps there are still a few Ar atoms incorporated in the sample microporous sites. Nevertheless, after being annealed at 85 K under 10^{-5} Pa, the surface of the ice must be free of argon contamination and is essentially made up of nanocrystalline clusters.[12,13]

Last, to test whether the thermal history affects ice surface thermodynamic properties, we choose to work with different types of ice samples: (i) amorphous sample prepared as previously described, annealed at 45 K and held at 43 K (referred to as surface S1); (ii) the same surface after evaporation of CO by pressure lowering and then annealed at 85 K (referred to as surface S2) to study at 43 K an eventual change in adsorption with a higher organized structure of the same sample; (iii) surfaces (labeled S3 and S4) deposited at 10 K and annealed at 85 K for 1 h but from different concentrations of the Ar/H_2O mixture (respectively 1/25 and 1/50) in order to check the reproducibility of the measurements; (iv) surface S5 prepared under the same condition as (i) but annealed at 110 K for 2 h.

As shown in Figure 1, the different thermal processes lead to surfaces corresponding to different degrees of crystal organization, the nonannealed sample (Figure 1d) being certainly less organized than the 160 K annealed one (Figure 1a).

Owing to the poor smoothing of the ice surface, it was impossible to measure their deposit thicknesses by interference spectra, and this parameter was more or less evaluated from the absorbances of the water vibrational modes given by the literature.[14] An estimate of these thicknesses is given in Table 2, column 3; however, this knowledge of the sample thickness is not essential for our data treatment.

For adsorption experiments, the substrate was cooled to the working temperature and the CO gas was introduced in the cryostat through a leak valve until the desired total dynamic pressure was reached. The CO gas (Air Liquide) is reported to have a chemical purity of 99.995% and is used without further

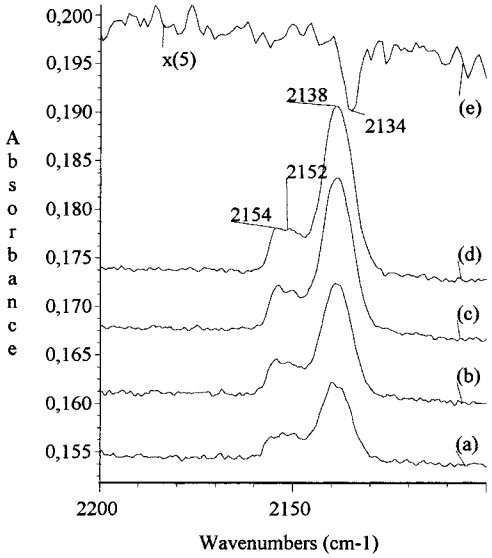

Figure 2. Selected fundamental mode spectra of carbon monoxide (CO) adsorbed on S3 ice surface at 43 K, plotted under different equilibrium pressures of CO: (a−f) spectra corresponding to 0.007, 0.029, 0.195, and 0.318 Pa. The 5 times expended difference spectrum (e) shows the remaining peak at 2134 cm^{-1}, which disappears only after a sample annealing at 140 K.

purification. The pressure was measured by a N_2 calibrated ion gauge. The upper pressure admitted in the cryostat must be less than 1 Pa to avoid accidental cooling of the infrared-transparent cryostat KBr windows. The CO gas injected 45° from the normal substrate must be partially thermalized at 77 K by collisions with the radiation shield walls before sticking onto the ice surface.

Between adsorption measurements the ice sample was maintained at 85 K to remove the adsorbed CO species and was continuously cleaned by an argon atomic beam under the cryostat base pressure (Ar vapor pressure is atmospheric at 87.1 K).

The infrared spectra were recorded on a Nicolet 7199 FTIR spectrometer equipped with a liquid nitrogen-cooled MCT detector, a Ge-coated KBr beam splitter, and a globar source. The resolution was set to 0.5 cm^{-1} without apodization, and the interpolation in the spectra was achieved by the zero filling method according to the spectral feature under examination. The integrated absorbances were measured as the area between a simulated line shape, giving a better fit to the experimental data and an extended baseline across the whole spectral range, using the FOCAS computer program of the Nicolet library.

2.2. Experimental Results. *2.2.1. Adsorption Spectra.* The spectra in Figure 2 show the fundamental band of $^{12}C^{16}O$ adsorbed on H_2O ice (substrate S3) as a function of pressure, the sample holder temperature being set at 43 K. The spectral features do not change too much in shape and frequency with increasing coverage within the experimental error limits (parts a and b of Figure 2). The shape also does not change with the organization of the substrate. It appears mainly as a multiplet whose minor components around 2154 and 2152 cm^{-1} lie on the shoulder of the strongest peak at 2138 cm^{-1} (fwhm $\approx$ 9 cm^{-1}). For a given temperature and pressure, the signal reaches its maximum value within a few minutes and remains stable. For a fixed substrate temperature all the infrared bands decrease with decreasing pressure while shape and frequency remain the same.

Because a weak peak centered at 2134 cm^{-1} is still visible in the spectrum (Figure 2e) after the pressure is lowered or even after the substrate is annealed to 85 K, adsorption and desorption processes do not appear to be completely reversible. Owing to the low working pressure range in which we accurately registered only the monolayer formation, it was impossible to observe any significant hysterisis process within the range of the experimental errors. We believe, however, that the remaining peak at 2134 cm^{-1} corresponds to CO absorbed by diffusion inside the substrate, showing its remaining porous character despite the annealing processes.

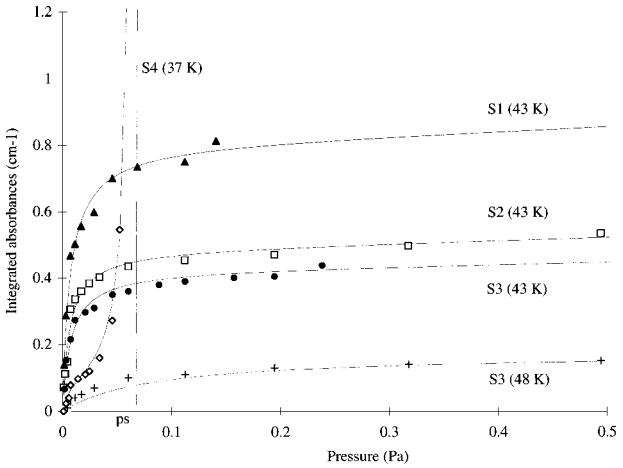

Figure 3. Adsorption isotherms for carbon monoxide (CO) on ice. The integrated absorbances of the fundamental vibrational mode of CO adsorbed on surfaces S1−S4 (see text) are reported against the equilibrium pressure of CO in Pa. The BET models have been drawn (solid lines) with a mean enthalpy of adsorption of the first monolayer and a BET net heat of adsorption equal to 10.0 and 2.3 kJ mol^{-1}.

The work most closely associated with our work has been that by Devlin,[15] and this point will be discussed later.

2.2.2. Isotherms. Figure 3 displays isotherms at different temperatures for four different ice samples. For each data point of an isotherm, the selected spectrum corresponds to the maximum and constant value of the infrared signal. Two isotherms at 43 K were recorded for two different organizations of the same ice sample (surfaces S1 and S2). The 43 and 48 K isotherms were measured for the same substrate (surface S3) previously annealed at 85 K.

To differentiate the monolayer or multilayer isotherm from that leading to the bulk CO solid, we measured an isotherm at 37 K for which the CO saturation pressure is about 0.06−0.08 Pa (Figure 3, surface S4). Besides a flat region corresponding to the formation of the first layers, it contains a growing region that corresponds to the solid formation at a limit pressure around 0.07 Pa. From this last experiment, we conclude that (i) the parameters pressure and temperature are measured with sufficient accuracy by our experimental procedure and (ii) the isotherm at 37 K can be related to type II isotherm. At higher temperature the isotherms are still of type II and correspond to the formation of the first monolayer followed by that of a few multilayer coverage.

Comparison between adsorption on S1 and S2 (Figure 3) at the same temperature shows clearly that the nonannealed sample presents a much larger specific area and consequently a lower degree of organization.

2.2.3. Adsorption Energies. In the Brunauer, Emmett, and Teller (BET)[16] model, adsorption occurs by the formation of stacks of particles on each surface adsorption site. If we call $-\epsilon$ the adsorption enthalpy of a molecule on the substrate at temperature T (first layer) and $-\epsilon'$ that corresponding to the adsorption on an already occupied site (subsequent layers), the

fractional coverage θ is defined as the ratio of the average number N of adsorbed species at pressure p by the monolayer capacity N_0. By use of a statistical model, θ is given by[17]

$$\theta = \frac{N}{N_0} = pp_0(T) \times \frac{1}{[p_0(T) + p - p\exp((\epsilon' - \epsilon)/kT)][p_0(T) - p\exp((\epsilon' - \epsilon)/kT)]} \quad (1)$$

In the low-pressure range, during the formation of the first layer, the behavior of the BET model is very similar to that of the Langmuir model. $p_0(T)$ is the pressure for which $\theta = {}^1/_2$ in a Langmuir isotherm

$$p_0(T) = \left(\frac{2\pi mkT}{h^2}\right)^{3/2} kT \exp\left(-\frac{\epsilon}{kT}\right) \quad (2)$$

where m is the molecular mass of CO considered as an ideal gas.

In the BET model the interactions between two adjacent adsorbed species are not taken into account in a first approximation. As a matter of fact, it seems to be a reasonable assumption for CO. Ab initio calculated interaction potential for CO···CO complexes of different shapes allows an evaluation of the binding energy to less than 2 kJ mol^{-1}.[18] This point will be examined from a more quantitative standpoint in the next section of this paper.

The evaluation of the energies from eq 1 requires a good determination of the fractional coverage θ. In eq 1, N is proportional to the integrated absorbance A:

$$A = \int_\Delta \ln\left(\frac{I_0}{I}\right) d\nu \quad (3)$$

The absorbance A_0, corresponding to N_0 available sites in the monolayer at completion, is experimentally deduced from the linear form of eq 1:

$$\frac{p}{A(p_s - p)} = \frac{1}{A_0 c} + \frac{c-1}{A_0 c}\frac{p}{p_s} \quad (4)$$

in which the parameter c is given by

$$c = \exp[-(\epsilon' - \epsilon)/(kT)] \quad (5)$$

and the saturation pressure p_s of the adsorbent, at temperature T, is related to $p_0(T)$ by

$$p_0(T) = p_s \exp[(\epsilon' - \epsilon)/(kT)] \quad (6)$$

For a given temperature, the parameters A_0 and $(\epsilon' - \epsilon)$ are obtained from relation 4. Their linear plots versus the ratio p/p_s are illustrated in Figure 4 for the S1, S2, and S3 surfaces at 43 K; the experimental data are very well fitted by the linear law.

Once A_0 has been determined, the coverage θ is calculated and the parameter $p_0(T)$ is deduced from eq 1 by its nonlinear optimization on the experimental data. The binding energy $-\epsilon$ is then calculated from eq 2. The results for the different samples are reported in Table 2 and illustrated in Figure 5. The mean binding adsorption enthalpy $-\epsilon$ between CO and the ice surface and the difference $-(\epsilon' - \epsilon)$ can be evaluated to be around 10.0 ± 0.3 and 2.3 ± 0.4 kJ mol^{-1}, respectively.

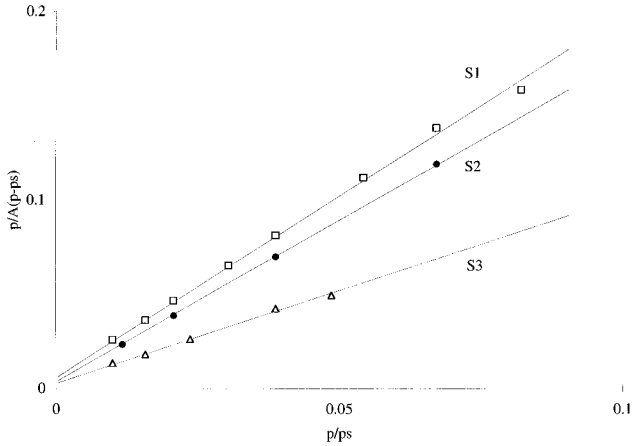

Figure 4. Experimental data fits by the linear form of the BET model.

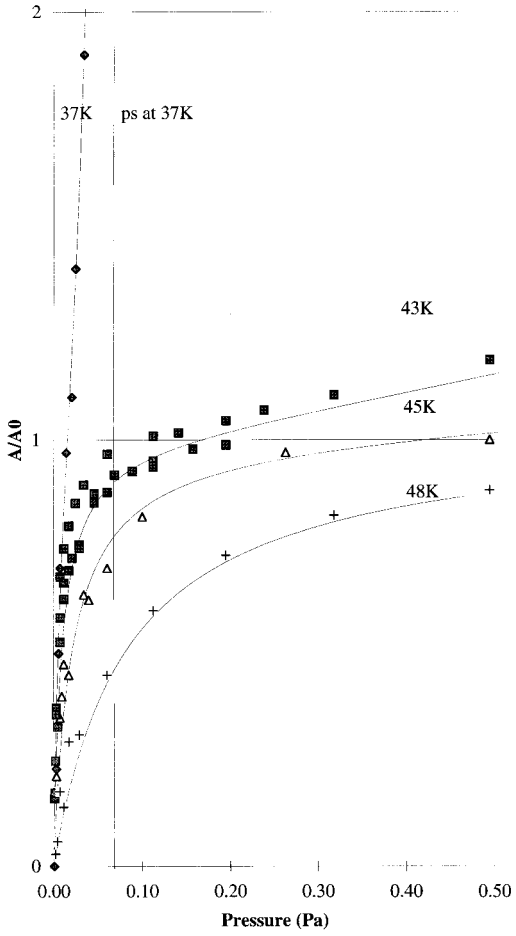

Figure 5. Surface coverage θ showing the multilayer formation at 37 K and the monolayer formation at 43, 45, and 48 K. The BET models have been drawn (solid lines) with the same parameters as in Figure 3.

The energy values in Table 2 lead to an energy of condensation of the adsorbate $-\epsilon'$ equal to 7.7 kJ mol^{-1}, which is comparable to the binding energy of CO in the solid state (8.9 kJ mol^{-1}). The BET isotherms in Figure 5 have been drawn with an enthalpy of adsorption of the first monolayer equal to 10.0 kJ mol^{-1} and a net heat of adsorption equal to 2.3 kJ mol^{-1}. These parameters are the mean values of data given in Table 2. The annealing process of the S1 sample leads to a 70% decrease of the monolayer capacity A_0, indicating a better surface organization.

From the good agreement between experimental data and

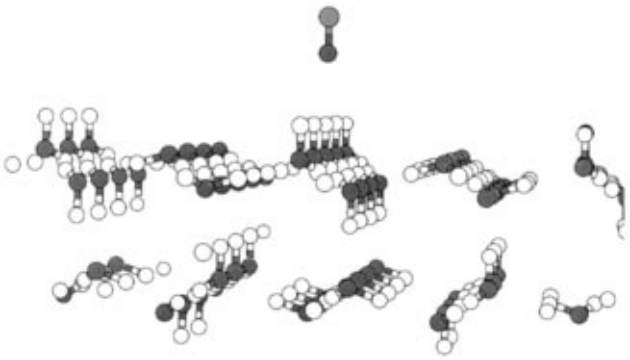

Figure 6. Representation of the slab used in the present study showing the dangling OH, the dangling oxygen atoms, the canals, and the carbon monoxide in the adsorption position.

BET model results (especially above 0.05 Pa) in the 43−48 K range, we infer the following.

(i) Within the range of the experimental errors on the absorbance, pressure, and temperature measurements, the adsorption energies are independent of temperature as postulated by the BET law. Note that in the 0.1−0.5 Pa range the error influence on the pressure measurement is less important.

(ii) The adsorption energies as well as the spectral shapes of the infrared signal do not depend upon the organization of the crystal within experimental error. This point will be developed in the discussion section.

3. Quantum Study

3.1. Method of Calculation. The quantum calculations of adsorption of small molecules made within the framework of the Hartree−Fock theory come under two main categories: (i) the cluster calculation in which the solid is calculated by a restricted number of molecules[19] and (ii) the periodic calculations[20] where the solid consists of a slab of infinite 2D layers. It has been shown in the above section that the ice surface that supported the experimental study presents a short-range ordered structure. This is the reason we chose the periodical representation: the potential exerted upon the CO molecule is certainly closer to a crystal type potential than to the potential generated by a restricted number of disordered water molecules. The present calculation is based on the ice structure as determined by Pisani et al.[4] This structure, referred to as P-ice by these authors and in the present paper, is derived from the ice XI structure and is of $Pna2_1$ symmetry. It was optimized using the CRYSTAL92[21,22] and EMBED93[23,24] computer programs. CRYSTAL92 is based on the periodic Hartree−Fock method, which solves the Schrödinger equation for crystals. It has been applied successfully to the study of different types of crystals involving hydrogen bonds. EMBED93 solves the defect problem by coupling Green's function of the host crystal to that of the defect (perturbed-cluster method[25]).

In the present work, the ice crystal is represented by a slab of two bilayers extracted from the bulk structure by cutting along the (001) surface without further relaxation or reorganization. In such a slab, the two faces are identical and there are no dipole moments between them that would introduce an instability factor. The (001) P-ice surface corresponds to the (0001) face of ice Ih as used by Materer et al.[3] These authors also defined a slab of bilayers and showed that cutting the crystal between two bilayers is 58 kJ mol^{-1} more stable than cutting within the bilayer because of the breaking of the hydrogen bonds. This model surface is characterized by the OH groups directed toward the outside of the system (dangling OH, Figure 6). The overlayer of the slab then consists of H atoms, providing for the stability and passivation of the surface. The dangling OHs are organized in parallel rows separated by 7.92 Å from each another. One hydroxyl group in a row is at 4.40 Å from its nearest neighbor in the same row. Alternating with the OH rows, the surface is occupied by oxygen atoms bonded to protons on the inside of the bulk (dangling oxygen). Above them electron density is high because of the oxygen lone pairs of electrons. Inside the bulk, linear structural canals of relatively large diameter are oriented parallel to the OH rows in the region between the two H_2O bilayers.

The adsorption energies ΔE_A are calculated for an isolated molecule (EMBED93) and for the adlayer (CRYSTAL92) by

$$\Delta E_A(\text{EMBED93}) = E(\text{ice} + \text{CO at } \infty) - E(\text{ice} + \text{adsorbed CO equilibrium}) \quad (7)$$

$$\Delta E_A(\text{CRYSTAL92}) = E(\text{ice}) + E(\text{CO isolated molecule}) - E(\text{ice} + \text{adsorbed CO equilibrium}) \quad (8)$$

In the latter case, there is one CO molecule per unit cell.

The chosen atomic basis set is the standard split valence Gaussian basis 6-31G, which was also used by Pisani et al. to determine the P-ice structure.[4] None of the two computer programs include the automatic energy gradient calculation. As a consequence, the equilibrium adsorption structures are calculated by quadratic interpolation techniques as already described elsewhere.[19] Preliminary tests allow us to conclude that the CO bond length does not vary significantly as the carbon monoxide is adsorbed. Then this parameter was kept at a fixed value throughout the calculations in order to limit the computation effort, which nevertheless remains important. These programs do not allow either the evaluation of the basis set superposition error (BSSE) or the dispersion forces. These two quantities will be evaluated by other methods and consequently other programs: the adsorption energies will be subsequently corrected from the EMBED calculation by the relation

$$\Delta E_A^{\text{Corr}} = \Delta E_A^{\text{EMBED}} + \Delta E^{\text{Disp}} + \Delta E^{\text{BSSE}} \quad (9)$$

3.1.1. BSSE Correction. In the perturbed cluster approach, Green's function of the admolecule and its immediate neighborhood (C zone in EMBED terminology) is calculated self-consistently; the crystal's Green's function (D zone) acts as a perturbation. Only the first zone is addressed by the BSSE. An approximate value of the BSSE is calculated using the usual counterpoise scheme[26] on the C zone, neglecting the crystal field. This is carried out by the GAUSSIAN94[27] computer package using the same Gaussian basis sets on CO and H_2O as in the EMBED calculation.

3.1.2. Dispersion Energy Calculation. If it were feasible to introduce the electronic correlation in CRYSTAL92 and EMBED93, the dispersion energy would have been taken into account in the Schrödinger equation provided diffuse enough orbitals are used and provided that these orbitals do not suffer from linear dependency. In the impossibility of undertaking such a calculation, the dispersion energy is evaluated by the electrostatic method.

Within the Buckingham electrostatic theory, the dispersion energy between two systems A and B is developed as a series of the inverse powers of the intersystems distance R:[28]

$$\Delta E^{\mathrm{Disp}} = U_{\mathrm{disp}}(R^{-6}) + U_{\mathrm{disp}}(R^{-7}) + U_{\mathrm{disp}}(R^{-8}) + U_{\mathrm{disp}}(R^{-9}) + \ldots \quad (10)$$

Limited to the first term, the dispersion energy averaged over all orientations becomes[29]

$$U_{\mathrm{disp}}(R^{-6}) = -\frac{C_6(\mathrm{A,B})}{R^6}$$

$$C_6(\mathrm{A,B}) = \frac{3}{\pi}\int_0^\infty \alpha^{\mathrm{A}}(\mathrm{i}\omega)\alpha^{\mathrm{B}}(\mathrm{i}\omega)\,\mathrm{d}\omega \quad (11)$$

α^{A} is the average diagonal component of the dynamic polarizability tensor.

Generally, the C_6 coefficients are either empirically extrapolated or calculated. In the present case, they are calculated by the time dependent Hartree−Fock theory (TDHF)[30] and the CADPAC[31] program package. This procedure does not introduce any empirical elements, and the calculation remains strictly within the quantum model.

The numerical value of the dispersion coefficients is very dependent upon the chosen atomic orbitals, and diffuse functions are of essential importance. The 6-31G basis is no longer sufficient. It must be extended to the 6-31++G(3df,2pd)[32] basis, adding d and p polarization functions[33] on C and O, p polarization function on H, d and f diffuse functions on C and O, and d and p diffuse functions on H.

The results are evaluated by comparing the first Cauchy moments with their experimental values. At low values of the real frequencies ω, the dynamical polarizability $\alpha(\omega)$ is expanded as a power of ω^2:

$$\alpha(\omega) = \sum_{k=0}^{\infty}(S_{-2k-2})\omega^{2k} \quad (12)$$

The first Cauchy moment $S(-2)$ is the static polarizability $\alpha(0)$.[29] In Tables 3 and 4 are reported our results compared to previous theoretical and experimental data concerning the homomolecular cases of interest: CO···CO and H_2O···H_2O. The C_6 coefficient corresponding to the CO···H_2O system is then calculated.

As will be shown in the next section, the intermolecular distances in the system under study are large enough to consider that the higher terms of the Buckingham series are negligible, especially considering that the dispersion energy calculated by this method is only an approximate corrective term.

The total dispersion energy is the sum of the interaction of the admolecule with the nearest water molecules (about 950 molecules). This contribution is always stabilizing.

3.1.3. CO···H_2O System in the Gas Phase. The geometry and interaction energy of carbon monoxide with a water molecule in vacuum are determined using the GAUSSIAN94 package at the HF/MP2 level and with the same extended 6-31++G(3df,2pd) basis set as previously described. The energies are corrected from the BSSE.

3.2. Quantum Results. *3.2.1. Adsorption on the Nondefective Surface.* By analogy with the CO/MgO[7,8,34] system, the first adsorption site we considered was located above a point of low electronic density, i.e., above a dangling hydrogen. The carbon monoxide axis was chosen to be perpendicular to the surface, and two cases were investigated: oxygen (scheme CO) or carbon (scheme OC) close to the surface. In Figure 7 are displayed the potential energy surfaces (PES) corresponding to these hypotheses and calculated using EMBED93 (uncorrected energies). In both cases the perturbed cluster involves the monoxide and the nearest water molecule.

The adsorption energies at the PES minimum are very similar in both cases, 10.7 kJ mol^{-1} in the CO scheme and 9.0 kJ mol^{-1} in OC, while the molecule−surface distances are, respectively, 2.17 and 2.30 Å.

As already observed by Pacchioni et al.[35] concerning the CO/MgO system, CO polarization has no noticeable incidence during adsorption on a site. Therefore, the HF error in the direction of the CO dipole moment should not have any consequence on the adsorption modeling.

The adsorption energy for the monolayer calculated by CRYSTAL92 and that for the same molecule−surface distance are very similar to those calculated using EMBED93, 9.9 and 10.2 kJ mol^{-1}, respectively, which must be compared with ϵ evaluated from the BET model in section 2.2.3. This highlights the good agreement between the periodic Hartree−Fock and the perturbed cluster methods as mentioned in a previous paper.[20] This result leads to a lateral interaction energy of about 1 kJ mol^{-1}. This very small value is a consequence of the large intermolecular distances between the adsorbed species on the surface; the CO molecules in the monolayer can be considered as independent from one another. This also comes as a posteriori justification for our using the BET model.

The associated vibrational frequencies ν_{CO} are also identical: 2319 and 2316 cm^{-1}. When CO is very far from the surface (10 Å), ν_{CO} calculated by the same method is equal to 2298 cm^{-1}. When the experimental value in the gas phase is 2133 cm^{-1}, the ratio of the experimental value to the theoretical value for the isolated monoxide is 0.93, very close to the scaling factor associated with a stretching mode according to the Pulay method.[36] We consider this result as a good test for the validity of the EMBED93 calculation concerning the frequencies calculation.[37]

The calculated adsorption energy must be corrected as indicated in sections 3.1.1 and 3.1.2. The dispersion correction is identical in both cases: +2 kJ mol^{-1}. The BSSE corrections are quite different. In the CO scheme, it compensates the former correction: −2 kJ mol^{-1}. However, in the OC orientation the BSSE correction is much higher: −6 kJ mol^{-1}. Obviously, this estimate does not take into account the crystal potential and must be considered as an overestimated value. Indeed, the electron density that diffuses toward the ghost orbitals in the counterpoise calculation is only 0.008 electron in the CO case and up to 0.024 electron in the OC case. In the latter case, this implies that the electrons borne by the oxygen atom tend to move toward the solid surface.

The corrected adsorption energies will be 10.9 kJ mol^{-1} when the monoxide's oxygen is next to the ice surface (CO) and 5.0 kJ mol^{-1} in the other case (OC). These corrected values are only estimates, and their level of accuracy is not high enough to differentiate the components of the infrared signals. It is then impossible to differentiate the two structures OC and CO on this particular point.

Other site structures have been investigated: (1) CO flat above one dangling OH and (2) CO or OC above a dangling oxygen, between two oxygen atoms, or above the hydrogen atoms in the surface portion between two OH rows. We even tried to adsorb a CO dimer flat above the surface or perpendicular to the surface. None of these hypotheses led to a stabilizing interaction. After these rather extensive investigations our conclusion is that the only adsorption site of the nondefective surface lies above the dangling hydroxyls.

3.2.2. Adsorption on a Model Defective Surface. The ice

TABLE 3: Calculated First Cauchy Moments Compared to Previous Work and Experiment (in au)

	$\alpha(0)$			$S(-4)$			$S(-6)$		
	this work	Spackman[29]	expt[a]	this work	Spackman[29]	expt[a]	this work	Spackman[29]	expt[a]
H_2O	8.299	8.018	9.642	21.366	22.54	35.42	104.616	107.61	240.1
CO	12.227	11.357	13.08	40.694	36.78	48.27	230.930	213.23	296.5

[a] Given by Spackman.

TABLE 4: Calculated C_6 Coefficients (in au)

	this work	Spackman[29]	expt
H_2O-H_2O	38.933	33.31	43.37
CO−CO	74.212	63.29	81.40
H_2O−CO	53.671		

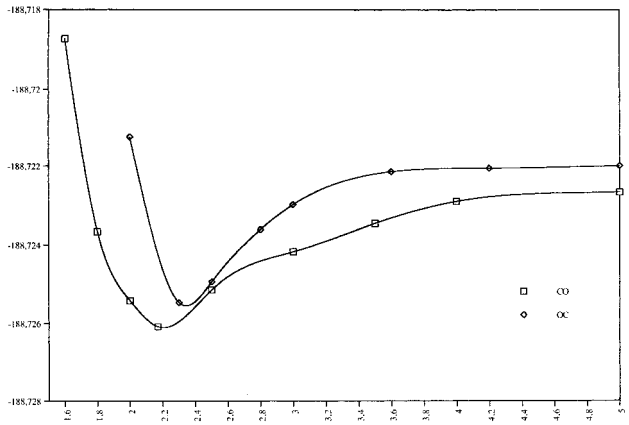

Figure 7. Potential energy surface corresponding to the two schemes of adsorption over the perfect surface. The units are hartrees for the energies and Å for the lengths.

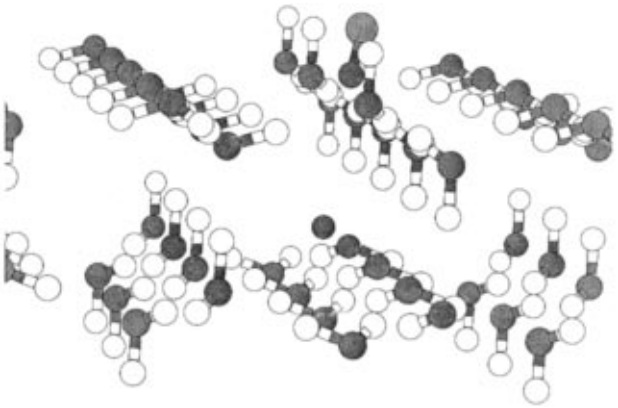

Figure 8. CO adsorption in a pore simulated by the absence of one water molecule.

surface as prepared for the spectroscopic measurements presents an ordered structure in local domains very large with respect to the CO molecule dimension. It probably presents also a large set of defects as dislocations and pores of various size. Modeling a pore is largely beyond our technical possibilities. Nevertheless, it is possible to simulate a pore by the hole generated by one water molecule extracted from the ice surface. As mentioned in the former subsection, the hole reconstruction was not considered because of computation time considerations. In this case, during adsorption, the monoxide's oxygen takes almost exactly the place of the missing water's oxygen (Figure 8). The corrected adsorption energy is then 44.3 kJ mol^{-1}, i.e., quite comparable to a hydrogen bond (the correction due to the BSSE is −5.7 kJ mol^{-1} and the dispersion contribution is +18.9 kJ mol^{-1}). The O···H distance, equal to 1.881 Å, is typically the length of a hydrogen bond. This value can be compared with the two hydrogen bond lengths in the P-ice structure, which are 1.747 and 1.802 Å. Such a high adsorption energy is also correlated to a rather large frequency shift for ν_{CO}: 2256 cm^{-1}. The inverted CO position has also been investigated but does not lead to a minimum in energy.

3.2.3. CO Diffusion Inside the Ice Canals. Considering that the ice crystal structure presents structural canals of relatively large diameters (section 3.1 and Figure 6) and that the monoxide is a small molecule, the hypothesis of molecular migration inside these structures must be taken into consideration.

Because of difficulties in SCF convergence in EMBED for this specific case, the calculation proceeds within the periodic HF framework. This option is consistent with the former section because of the large crystal unit cell and because the lateral interactions between admolecules are negligible.

The slab size (two bilayers) does not allow consideration of the canal distortion in the neighborhood of the migrating CO. The CRYSTAL calculation then assumes that the two subsystems CO and ice remain unchanged. The interaction energy is calculated by the same formula as that used for the adsorption energy.

Among the numerous structures we studied, the least unfavorable corresponds to the monoxide nearly perpendicular to the two slab surfaces, at equal distance from the two, and in the middle of the unit cell. Nevertheless, the total energy of this system is 78 kJ mol^{-1} higher than the sum of the uncorrected energies of the two subsystems. This amount of energy is so important that it is highly improbable it could be compensated for reconstruction of the canal.[38] It must be concluded that the carbon monoxide cannot migrate inside the ice canals. Indeed, the experimental ice sample is far from a perfect monocrystal and migration between crystallites is probable, as we already mentioned in subsection 2.2.2. The molecule must be trapped in large holes, and its vibrational mode is probably not affected by the short-range surface interaction.

3.2.4. H_2O···CO Interaction in Vacuum. At this stage of the study a first conclusion is that two sorts of monoxide interactions are possible with the ice surface: a weak interaction within the range 5−10 kJ mol^{-1} and hydrogen bond type interaction (around 40 kJ mol^{-1}) correlated to a strong lowering to the fundamental vibrational mode when the surface structure is perturbed by hole type defects. These results are to be compared with the behavior of the same molecules when they are not embedded in the ice crystal surface.

The system CO···H_2O corresponds to a BSSE-corrected energy of 5.0 kJ mol^{-1} and a O···H distance of 2.333 Å. The complex OC···H_2O corresponds to an energy of 5.9 kJ mol^{-1} and a C···H distance of 2.422 Å. In both cases no minimum was found that would correspond to hydrogen bond. It must also be noted that the interaction of water with carbon is more stabilizing than with oxygen, in contrast to adsorption on ice.

The interaction of water with two monoxide molecules gives very similar results: 11.7 kJ mol^{-1} for the OC···H_2O···CO system, the C···H distance being 2.4441 Å, and 8.8 kJ mol^{-1} for the OC···H_2O···OC system, with O···H being 2.404 Å and C···H 2.424 Å.

It ensues from these calculations that in the gas phase, the hydrogen bond seems to be impossible between water and carbon monoxide and only weak bonds of the van der Waals type are present. The associated bond energies are quite comparable to the adsorption energies we found on a perfect ice surface. As a consequence, we deduce that the hydrogen bond stabilization of the system is only ascribable to the crystal field perturbation generated by the hole in the surface.

4. Discussion and Conclusion

The physical problem this quantum calculation aims to model lies in the use of the infrared spectral signature of the adsorbed CO to measure the adsorption energy and to probe the surface substrate by thermodynamic measurements.

The work closely associated with our study in infrared spectroscopy has been made by Devlin[15] who assigned the band around 2152 cm^{-1} to CO in interaction with the dangling OH groups. The band at 2138 cm^{-1} was described as a "normal mode" according to the experimental data reported in the literature for CO in solid-state or argon matrixes.[39] In our own experiment the component around 2152 cm^{-1} and the stronger peak at 2138 cm^{-1} grew similarly, with the surface coverage preserving the spectral shape and peak frequencies. In our opinion this fact indicates clearly that these peaks correspond to different but very similar adsorption sites.

The quantum calculations indicate (within the general framework of our hypothesis) the following.

(i) If the ice surface was perfect, then two types of adsorption must be possible: the CO and the OC schemes above a dangling OH. The molecule−surface interaction energy is about 10 kJ mol^{-1} for the two orientations on the adsorption site. Nevertheless, if we take into account the basis set superposition error and the approximate dispersion contribution, it seems that the conformation when the oxygen is near the ice surface is less stable than the other conformation. Although we are not able to distinguish experimentally between the two sites regarding the CO vibration frequencies, it can be reasonably expected that they cannot be very different. We can also affirm that no other adsorption site is present on the perfect surface.

(ii) If the surface shows defects such as holes, then the electrostatic potential inside the hole is strong enough to induce more stabilizing bonds between the molecule and the surface. The adsorption energy is then 44.3 kJ mol^{-1}, at least 4 times greater than the former energies.

Qualitatively, the size of the hole is not fundamental. It is well-known, for example, that the "active" part of a crystal defect (such as a step or a kink) is the edge. In the same manner, the "active" part of the hole is the edge,[40] whatever the size of the hole.

If we choose the hypothesis that one of the spectral components corresponds to a weak interaction and the second to a stronger one, then the energy difference is too high to cause the two peaks to grow in parallel and the calculated frequency shift does not correspond to the observed one, even qualitatively. It is well-known that the HF frequency calculation suffers from systematic errors, but here, we are discussing frequency differences instead of absolute values, and the calculated difference is in good agreement with what could be expected from the physical situations.

The unique hypothesis that is consistent with our experimental observations, within the experimental errors, is to assign the doublet (2152 and 2138 cm^{-1}) to two sites corresponding to CO and OC adsorption above the dangling OH groups.

The calculation we made on the OC···H_2O···CO and OC···H_2O···OC systems is consistent with Lundell et al.'s.[41] Moreover, these authors also calculated the CO vibration frequencies. In the OC···H_2O···OC system, the two frequencies are 15.6 cm^{-1} apart. This value corresponds exactly to the split observed on ice.

Sadlej et al.[42] have also investigated the CO···H_2O system. Although they were able to use a much more sophisticated method than ours, their results are in good agreement with the present study. The interaction energies of CO···H_2O and OC···H_2O are, respectively, 1.4 and 2.4 kJ mol^{-1} without CP-geometry correction and 7.3 and 2.8 kJ mol^{-1} with CP-geometry correction. This point strongly indicates the utmost sensitivity of this system to the basis set superposition error, which, in this case, more dramatically disturbs the CO···H_2O system as opposed to its equivalent on ice. The CO stretch frequencies are calculated as 2104 and 2090 cm^{-1} respectively. This last point reinforces our assumptions, since a difference of about 5 kJ mol^{-1} in energy induces a frequency splitting of 14 cm^{-1}, i.e., the same order of magnitude that we observed for the CO/ice system.

Carbon monoxide is a molecule with a very weak dipole moment and is not very hydrophilic. Its adsorption on ice cannot induce significant perturbations of the surface. Thus, it is possible to draw some tentative conclusions about the surface structure that are supported by our experimental results.

If the surface is perfect and perfectly plane, no strong coupling is possible with CO. In the real situation the ice sample is far from perfect; the surface presents defects and pores. We have shown that the CO-model defect interaction energy is much higher (44 kJ mol^{-1}) than the measured one (10 kJ mol^{-1}). We must then consider that the ice surface is passivated by the dangling OHs to such an extent that CO adsorption occurs, in accordance with our weak interaction model, as on an ideal surface despite the defects. This phenomenon is certainly exhausted by the large vibrational amplitudes of the first ice layer, which, according to Van Hove's results,[3a] continue to exist even at low temperature. The two mean infrared bands that grow and decrease in an identical way are associated with physically analogous adsorption sites.

The thermal treatments applied on the surface sample aim to obtain a nanocrystalline solid that is characterized by its spectral signature. Whatever is the degree of organization of the surface, neither the number nor the position and shape of the peaks are affected, in contradiction with Devlin's studies on CF_4 adsorption on ice.[5f] Here, the situation is qualitatively different. The CF_4 molecule is strongly hydrophobic and the preferential adsorption site is inside the *hexagonal ice surface structure*, whereas CO adsorbs preferentially on dangling OH. The CF bonds are more polarized than CO, and the collective behavior leads to a coupling between admolecules by strong lateral interaction. This induces vibrational excitation of the ν_3 mode that resembles transverse−longitudinal (T−L) splitting that is very sensitive to the surface organization even in at low coverage. Such a coupling is not observed for a monolayer of CO either on ionic surfaces[8b] or in our experiments.

The mean net heat of adsorption ΔQ_{CO} equal to 2.3 kJ mol^{-1} (from column 6 in Table 2) is halfway between that of N_2 adsorbed on different ice surfaces[12,13] ($\Delta Q_{N_2} = 2.7$ kJ mol^{-1}) and that of CH_4[43] ($\Delta Q_{CH_4} = 1.95$ kJ mol^{-1}). Indeed, CO and N_2 are essentially characterized by their quadrupole moments and interact preferentially with the dangling OH groups. But the spherical CH_4 molecule, not presenting any electrostatic moments, interacts via dispersion type forces not only with the

dangling OH but also with all the different components of the ice surface. Nevertheless, in all the cases, at coverages corresponding to about one monolayer, the net heat of adsorption appears to be independent both of the type of interaction and of the ice surface organization. However, at low coverage ΔQ_{CH_4} is strongly dependent on the surface, thus making it a good candidate for probing the defects on the surface. The poor sensitivity of infrared spectroscopy at low coverages (see, for instance, the spread of the data values at 43 K under $\theta = 1$ in Figure 5) does not allow any further comparison.

In a recently published paper, Schaff and Roberts[6f] reported on the adsorption of small molecules on thin ice films, whether amorphous or crystalline. They concluded that if the surface were porous, the trapping pores would increase significantly the activation barrier of desorption, and our quantum study reinforces this assumption concerning the similarity of the components of the doublet at 2138 and 2152 cm^{-1}. Moreover, the peak intensities corresponding to the stretching OH modes would be modified, since the response of the hydroxyls inside the pores is different from those of the surface. However, we did not observe these points.

These arguments lead to the same conclusion: the ice surface we accurately observe around the formation of the first monolayer is reconstructed in such a manner that all the dangling hydroxyls are equivalent; the carbon monoxide cannot see any trapping defect on the surface (not considering the weak signal remaining at 2134 cm^{-1} that we definitively attribute to CO trapped in a cage inside the bulk). The mean enthalpy of adsorption of the first monolayer can be reasonably evaluated, from infrared spectroscopy, to be about 10 kJ mol^{-1}.

So infrared spectroscopy, already widely used for determining the structure of molecules adsorbed onto a large variety of surfaces, may also be used to calculate thermodynamic quantities concerning the nature of the interaction between the admolecule and the substrate. Though not as good as standard volumetric methods to obtain low-noise adsorption isotherms, especially for low surface coverage of the substrate, it conveniently gives data in the spectroscopic and thermodynamic domains for the same sample under similar physical constraints. Presently this method allows us to conclude the existence of two sites of adsorption of CO on ice with equivalent interaction energies.

Acknowledgment. The authors are greatly indebted to Professor F. Rouquerol for helpful discussions. These calculations were carried out at the CNRS Computer Center IDRIS (Institut du Développement et des Ressources en Informatique Scientifique).

References and Notes

(1) E-mail: allouche@piimsdm11.univ-mrs.fr.

(2) See, for example, the following. (a) Solomon, S. *Rev. Geophys.* **1988**, *26*, 131. (b) Molina, M. J.; Tos, T.-L.; Molina, L. T.; Wang, F. C. *Science* **1987**, *238*, 1253. (c) Clary, D. C. *Science* **1996**, *271*, 1509. (d) Gertner, B. J.; Hynes, J. T. *Science* **1996**, *271*, 1563.

(3) (a) Materer, N.; Starke, U.; Barbieri, A.; van Hove, M. A.; Somorjai, G. A.; Kroes, G.-J.; Minot, C. *J. Phys. Chem.* **1995**, *99*, 6267. (b) Materer, N.; Starke, U.; Barbieri, A.; van Hove, M. A.; Somorjai, G. A.; Kroes, G.-J. Minot, C. *Surf. Sci.* **1997**, *381*, 190.

(4) (a) Pisani, C.; Casassa, S.; Ugliengo, P. *Chem. Phys. Lett.* **1996**, *253*, 201. (b) Casassa, S.; Ugliengo, P.; Pisani, C. *J. Chem. Phys.* **1997**, *106*, 8030.

(5) (a) Silva, S. C.; Devlin, J. P. *J. Phys. Chem.* **1994**, *98*, 10847. (b) Sadlej, J.; Rowland, B.; Devlin, J. P.; Buch, V. *J. Chem. Phys.* **1995,** *102*, 4804. (c) Rowland, B.; Kadagathur, N. S.; Devlin, J. P. *J. Chem. Phys.* **1995**, *102*, 8328. (d) Fisher, M.; Devlin, J. P. *J. Phys. Chem.* **1995**, *99*, 11584. (e) Devlin, J. P.; Buch, V. *J. Phys. Chem.* **1995**, *99*, 16534. (f) Buch, V.; Delzeit, L.; Blackledge, C.; Devlin, J. P. *J. Phys. Chem.* **1996**, *100*, 3732.

(6) (a) Schaff, J. E.; Roberts, J. T. *J. Phys. Chem.* **1994**, *98*, 6900. (b) Graham. J. D.; Roberts J. T. *J. Phys. Chem.* **1994**, *98*, 5974. (c) Blanchard, J. L.; Roberts, J. T. *Langmuir* **1994**, *10*, 3303. (d) Graham, J. D.; Roberts, J. T. *Geophys. Res. Lett.* **1995**, *22*, 251. (e) Graham, J. D.; Roberts, J. T. *J. Phys. Chem.* **1994**, *98*, 5974. (f) Schaff, J. E.; Roberts, J. T. *J. Phys. Chem.* **1996**, *100*, 14151.

(7) (a) Casanovas, J.; Pacchioni, G. *Chem. Phys. Lett.* **1996**, *259*, 438. (b) Jaffe, J. E.; Hess, A. C. *J. Chem. Phys.* **1996**, *104*, 3348. (c) Ferullo, R. M.; Castellani, N. J. *Langmuir* **1996**, *12*, 70. (d) Gruver, V.; Fripiat, J. J. *J. Phys. Chem.* **1994**, *98*, 8549. (e) Skelton, D. C.; Wei, D. H.; Kevan, S. D. *Surf. Sci.* **1994**, *320*, 77. (f) Fahmi, A.; Minot, C. *J. Organomet. Chem.* **1994**, *478*, 67. (g) Richardson, N. V.; Bradshaw, A. M. *Surf. Sci.* **1979**, *88*, 255.

(8) (a) Hoang, P. N. M.; Picaud, S.; Girardet, C. *J. Chem. Phys.* **1996,** *105*, 8453. (b) Chang, H. C.; Richardson, H. H.; Ewing, G. E. *J. Chem. Phys.* **1988**, *89*, 7561. (c) Briquez, S.; Girardet, C.; Goniakowski, J.; Noguera, C. *J. Chem. Phys.* **1996,** *105*, 678. (d) Picaud, S.; Hoang, P. N. M.; Girardet, C. *Surf. Sci.* **1993**, *294*, 149. (e) Nygren, M. A.; Petterson, L. G. M.; Barandia, Z.; Seijo, L. *J. Chem. Phys.* **1993**, *100*, 2010. (f) Nygren, M. A.; Petterson, L. G. M. *J. Chem. Phys.* **1996**, *105*, 9339. (g) Marchese, L.; Coluccia, S.; Martra, G.; Zecchina, A. *Surf. Sci.* **1992**, *269*/*270*, 135. (h) Colbourn, E. A.; Mackrodt, W. C. *Surf. Sci.* **1984**, *143*, 391. (i) Pacchioni, G.; Neyman, K. M.; Rösch, N. *J. Electron Spectrosc. Relat. Phenom.* **1994**, *69*, 13. (j) Pacchioni, G.; Minerva, T.; Bagus, P. S. *Surf. Sci.* **1992**, *275*, 450. (k) Minot, C.; van Hove, M. A.; Biberian, J.-P. *Surf. Sci.* **1995**, *346*, 283. (l) Neyman, K. M.; Ruzankin, S. P.; Rösch, N. *Chem. Phys. Lett*. **1995**, *246*, 546. (m) Tashiro, T.; Ito, J.; Sim, R.-B.; Miyazawa, K.; Hamada, E.; Toi, K.; Kobayashi, H.; Ito, T. *J. Phys. Chem.* **1995**, *99*, 6115. (n) Mejias, J. A.; Marquez, A. M.; Ferdandez-Sanchez, J.; Ferdandez-Garcia, M.; Ricart, J. M.; Sousa, C.; Illas, F. *Surf. Sci.* **1995**, *327*, 59. (o) Katrin, K. J.; Albert, K.; Gerwens, H. *J. Chem. Phys.* **1995**, *101*, 11060.

(9) Neyman, K. M.; Strodel, P.; Ruzankin, S. P.; Schlensog, N.; Knözinger, H Rösch, N. *Catal. Lett.* **1995**, *31* , 273.

(10) (a) Fredin, L.; Nelander, B.; Ribbegard, G. *J. Chem. Phys.* **1977**, *66*, 4065. (b) Bentwood, R. M.; Barnes, A. T.; Orville-Thomas, W. J. *J. Mol. Spectrosc*. **1980**, *84*, 391.

(11) (a) Rowland, B.; Fisher, M.; Devlin, J. P. *J. Chem. Phys.* **1991**, *95*, 1378. (b) Buch, V.; Devlin, J. P. *J. Chem. Phys.* **1991**, *94*, 4091.

(12) Schmitt, B.; Ocampo, J.; Klinger, J. *J. Phys.* **1987**, *48-C1*, 519.

(13) Chaix, L.; Ocampo, J.; Dominé, F. *C. R. Acad. Sci. Paris, Ser. IIa* **1996**, *322*, 609.

(14) Bergren, M. S.; Schuh, D.; Sceats, M. G.; Rice, S. *J. Chem. Phys.* **1978**, *69*, 3477.

(15) Devlin, J. P. *J. Phys. Chem.* **1992**, *96*, 6185.

(16) Brunauer, S.; Emmet, P. W.; Teller, E. J. *J. Am. Chem. Soc.* **1938**, *60*, 309.

(17) Desjonquères, M. C.; Spanjaard, D. *Concepts in Surface Physics*; Springer-Verlag: Berlin, 1993.

(18) van der Pol, A.; van der Avoird, A.; Wormer, P. E. S. *J. Chem. Phys.* **1990**, *92*, 7498.

(19) Allouche, A. *J. Phys. Chem.* **1996**, *100*, 1820, 17915.

(20) (a) Ferro, Y.; Allouche, A.; Corà, F.; Pisani, C.; Girardet, C. *Surf. Sci.* **1995**, *325*, 139. (b) Allouche, A. *Surf. Sci.* **1997**, *374*, 117.

(21) Pisani, C.; Dovesi, R.; Roetti, C. *Hartree-Fock ab initio treatment of crystalline systems*; Lecture Notes in Chemistry 48; Springer: Berlin, 1988.

(22) Dovesi, R.; Saunders, V. R.; Roetti, C.; Causà, M.; Harrison, N. M.; Orlando, R.; Aprà, E. CRYSTAL95 User's Manual; Universitàdi Torino, 1996.

(23) Pisani, C.; Corà, F.; Nada, R.; Orlando, R. *Comput. Phys. Commun.* **1994**, *82*, 139. Pisani, C.; Birkenheuer, U. *Comput. Phys. Commun.* **1996**, *96*, 152.

(24) Pisani, C.; Corà, F.; Nada, R.; Orlando, R. EMBED93 User's Manual; Universitàdi Torino, 1993.

(25) Pisani, C. *Quantum Mechanical Ab-initio Calculation of the Properties of Crystalline Materials*; Lecture Notes in Chemistry 67; Springer-Verlag: Berlin, 1996.

(26) Boys, S. F.; Bernardi, F. *Mol. Phys.* **1970**, *19*, 553.

(27) Frisch, M. J.; Trucks, G. W.; Schlegel, H. B.; Gill, P. M. W.; Johnson, B. G.; Robb, M. A.; Cheeseman, J. R.; Keith, T.; Petersson, G. A.; Montgomery, J. A.; Raghavachari, K.; Al-Laham, M. A.; Zakrzewski, V. G.; Ortiz, J. V.; Foresman, J. B.; Cioslowski, J.; Stefanov, B. B.; Nanayakkara, A.; Challacombe, M.; Peng, C. Y.; Ayala, P. Y.; Chen, W.; Wong, M. W.; Andres, J. L.; Replogle, E. S.; Gomperts, R.; Martin, R. L.; Fox, D. J.; Binkley, J. S.; Defrees, D. J.; Baker, J.; Stewart, J. P.; Head-Gordon, M.; Gonzalez, C.; Pople, J. A. *Gaussian 94*, Revision C.2; Gaussian, Inc.: Pittsburgh, 1995.

(28) Buckingham, A. D. *Adv. Chem. Phys.* **1967**, *12*, 107.

(29) Spackman, M. A. *J. Chem. Phys.* **1991**, *94*, 1288, 1295.

(30) Amos, R. D.; Handy, N. C.; Knowles, P. J.; Rice, J. E.; Stone, A. J. *J. Phys. Chem.* **1985**, *89*, 2186.

(31) Alberts, I. L.; Andrews, J. S.; Colwell, S. M.; Handy, N. C.; Jayatalaka, D.; Knowles, P. J.; Kobayashi, R.; Laidig, K. E.; Laming, G.;

Lee, A. M.; Maslen, P. E.; Murray, C. W.; Rice, J. E.; Simandiras, E. D.; Stone, A. J.; Su, M.-D.; Tozer, D. J. *CADPAC: The Cambridge Analytic Derivatives Package Issue 6*; Cambridge, U.K., 1995.

(32) (a) Hehre, W. J.; Ditchfield, R.; Pople, J. A. *J. Chem. Phys.* **1972**, *56*, 2257. (b) Hariharan, P. C.; Pople, J. A. *Theor. Chim. Acta* **1973**, *28*, 213. (c) Gordon, M. S. *Chem. Phys. Lett.* **1980**, *76*, 163.

(33) Clark, T.; Chandrasekhar, J.; Spitznagel, G. W.; Schleyer, P. V. R. *J. Comput. Chem.* **1983**, *4*, 294.

(34) (a) Causà, M.; Kotomin, E.; Pisani, C.; Roetti, C. *J. Phys. C: Solid State Phys.* **1987**, *20*, 4991. (b) Dovesi, R.; Orlando, R.; Ricca, F.; Roetti, C. *Surf. Sc*i. **1987**, *186*, 267. (c) Neyman, K. M.; Rösch, N. *Ber. Bunsen-Ges. Phys. Chem.* **1992**, *96*, 1711. Neyman, K. M.; Rösch, N. *Chem. Phys.* **1992**, *168*, 267. Neyman, K. M.; Rösch, N. *Surf. Sci.* **1993**, *297*, 223. (d) Neyman K. M.; Ruzankin, S. Ph.; Rösch, N. *Chem. Phys. Lett.* **1995**, *246*, 546.

(35) Pacchioni, G.; Cogliandro, G.; Bagus, P. S. *Int. J. Quantum Chem.* **1992**, *42*, 1115.

(36) Fogarasi, G.; Pulay, P. In *Ab initio calculation of force fields and vibrational spectra*; Vibrational Spectra and Structure 14; Durig, J. R., Ed.; Elsevier: Amsterdam, 1985.

(37) Allouche, A.; Corà, F.; Girardet, C. *Chem. Phys.* **1995**, *201*, 59.

(38) Pisani, C. Private communication.

(39) Jiang, G. J.; Person, W. B.; Brown, K. G. *J. Chem. Phys.* **1975**, *62*, 1201.

(40) Anchell, J. L.; Hess, A. C. *J. Phys. Chem.* **1996**, *100*, 18317.

(41) Lundell, J.; Räsänen, M.; Latajka, Z. *Chem. Phys. Lett.* **1994**, *222*, 33.

(42) Sadlej, J.; Buch, V. *J. Chem. Phys.* **1994**, *100*, 4272.

(43) *Gas Encyclopedia*; Elsevier: Amsterdam, 1976.

(44) Clayton, J. O.; Giauque, W. F. *J. Am. Chem. Soc.* **1932**, *54*, 2610. Angerand, F. Thèse d'Université Nancy I, France, 1987.

(45) Chaix, L.; Dominé, F. *J. Phys. Chem. B.* **1997**, *101*, 6105.